

Physics Backgrounds to Supersymmetric Signals with Two Photons and Missing Mass at LEP

S. Mrenna[*]
High Energy Physics Division
Argonne National Laboratory
Argonne, IL 60439

August 14, 2017

Abstract

We calculate the event rates for the Standard Model production of two photons plus missing mass through the process $e^+e^- \rightarrow \gamma\gamma\nu\bar{\nu}$, where ν is any of the three neutrino flavors. This process can be a background to new physics signatures, such as that expected from supersymmetry with a higgsino or gravitino LSP. The missing mass spectrum is presented for several sets of kinematic cuts at $\sqrt{s}=161, 172, 184, \text{ and } 194$ GeV. The effect of initial state photon radiation is also studied, and is found to be significant, approximately doubling the event rates.

1 Introduction

The general case for weak scale supersymmetry has been reviewed in Ref.[1]. Recently, some evidence has accumulated that is consistent with a light supersymmetric particle spectrum containing a lightest superpartner (LSP) that is the lightest neutralino \tilde{N}_1 with a high higgsino content[2]. In such models, a photino-like neutralino \tilde{N}_2 can decay $\tilde{N}_2 \rightarrow \tilde{N}_1\gamma$, where \tilde{N}_1 escapes the detector. Direct pair production of \tilde{N}_2 or the indirect pair production from the decays of sneutrino pairs, $\tilde{\nu}(\rightarrow \tilde{N}_2\nu)$, can lead to a striking signature $\gamma\gamma M$, where M is missing mass. Such signatures are also possible from neutralino production and decay for a gravitino LSP \tilde{G} , e.g. $e^+e^- \rightarrow \tilde{N}_1(\rightarrow \gamma\tilde{G})\tilde{N}_1(\rightarrow \gamma\tilde{G})$, in models of gauge mediated supersymmetry breaking[3]. See also the references [4].

In the Standard Model, similar final states can arise from the process $e^+e^- \rightarrow \gamma\gamma\nu\bar{\nu}$. When $\nu = \nu_\mu, \nu_\tau$, the neutrinos are produced through a Z boson resonance. Hence, the M distribution has a characteristic shape peaked at M_Z . However, when $\nu = \nu_e$, there are additional contributions from virtual W

bosons. As a result, the ν_e process acquires a tail in the M distribution far from the Z boson mass.

The purpose of this report is to quantify the Standard Model rate for $\gamma\gamma M$ events, so that one can address the significance of any such events with large M .

2 Calculation and Results without Initial State Radiation

The cross section for the process $e^+e^- \rightarrow \gamma\gamma\nu\bar{\nu}$ is calculated using the helicity amplitude library HELAS[5] to evaluate amplitudes derived by the program Madgraph[6]. The inputs to the program are $\alpha = .0078$, $\sin\theta_W = .230$, $M_W = 80$ GeV, $\Gamma_W = 1.903$ GeV, $M_Z = 91.17$ GeV, and $\Gamma_Z = 2.288$ GeV. The calculation is done at a fixed order, with two and only two hard photons in the final state. The effect of undetected initial state radiation is considered in Sec. 3.

Based on the analysis presented by the OPAL collaboration[7], we require that both photons satisfy $|\cos\theta| < .7$, where θ is the photon angle with respect to the beam axis in the laboratory frame, and $E^\gamma > E_{\min}^\gamma$, where E^γ is the photon energy. We study the sensitivity of the event rate and distributions to the choices $E_{\min}^\gamma = 1.75, 5, \text{ and } 10$ GeV and to another cut on $|\cos\theta|$.

Our results are summarized in Figures 1–4. In Fig. 1, we present the missing mass distribution in pb per GeV bin for a minimum photon energy of 1.75 GeV at $\sqrt{s} = 161, 172, 184, \text{ and } 194$ GeV. The missing mass M is defined to be the invariant mass of the four vector $(p_{e^+} + p_{e^-} - p_{\gamma_1} - p_{\gamma_2})^\mu$. For $M < 80$ GeV, the cross section is negligible. The integrated cross section for $M > 100$ GeV is also shown in the figure. For the machine energies considered, this number is almost a constant, about .016 pb. Figs. 2 and 3 show the same distributions for $E_{\min}^\gamma = 5$ and 10 GeV respectively. The integrated cross section for $M > 100$ GeV is roughly .007 and .003 pb for the two cuts regardless of the beam energy. Finally, Fig. 4 shows the correlation between the two photon energies in pb per GeV^2 bin at $\sqrt{s} = 161$ GeV. There is a peak when both photons are soft, and a ridge for one soft and one hard photon. Away from this region, the distribution is fairly flat.

If, instead, we require $|\cos\theta| < .95$, the results are similar, except that the event rate is higher. For $E_{\min}^\gamma = 1.75, 5, \text{ and } 10$ GeV, the integrated cross section for $M > 100$ GeV is roughly .074, .033, and .016 pb regardless of the beam energy. These numbers are in agreement with an independent calculation[8]. Therefore, there is a substantial gain in reducing the Standard Model contribution to $\gamma\gamma M$ events by focussing on the central region of the detector.

3 Calculation and Results with Initial State Radiation

In principle, the colliding e^+ and e^- need not each have the beam energy, but may have radiated many undetected photons beforehand. The effect of undetected initial state radiation is to reduce the center of mass energy closer to M_Z and to generate a component of missing momentum down the beampipe. The increasing partonic cross section must be folded with the decreasing probability that the incoming e^- (e^+) carries a reduced fraction of the beam energy. In QED, the electron momentum distribution functions are entirely calculable, and depend on the inputs α ($\simeq 1/137$), m_e , and the beam energy. We use the next-to-leading-order exponentiated form as described in Ref.[9] and implemented in the PYTHIA subroutine PYPDEL[10].

The effect of undetected initial state photon radiation is illustrated in Figs. 5–8. In Fig. 5, we present the missing mass distribution in pb per GeV bin for a minimum photon energy of 1.75 GeV at $\sqrt{s}=161, 172, 184,$ and 194 GeV. The integrated cross section for $M > 100$ GeV at $\sqrt{s} = 161$ GeV is .035 pb, or more than double the previous estimate without initial state radiation. This rate decreases slightly for higher beam energies. Figs. 6 and 7 show the same distributions for $E_{\min}^\gamma=5$ and 10 GeV respectively. The integrated cross section for $M > 100$ GeV is roughly .016 and .008 pb for the two cuts regardless of the beam energy, also about double the previous estimate. Finally, Fig. 8 shows the correlation between the two photon energies in pb per GeV^2 bin at $\sqrt{s}=161$ GeV.

If $|\cos\theta| < .95$, the integrated cross section for $M > 100$ GeV is roughly .155, .076, and .035 pb at $\sqrt{s} = 161$ GeV for $E_{\min}^\gamma=1.75, 5,$ and 10 GeV, respectively. As for the case of harder cuts, the rates are about double when including initial state radiation.

Note that such calculation should not be trusted when one or both of the photons are very soft. In that case, multiple soft photon emission will be important. Likewise, event generators for a single hard photon and soft photons should not be used to estimate the rate for two hard photons. Finally, other potential Standard Model contributions to the $\gamma\gamma M$ final state are $e^+e^- \rightarrow \gamma\gamma e^+e^-$, where both the electron and positron are undetected in the beam pipe, or $e^+e^- \rightarrow \gamma\gamma X$, where X is any number of undetected photons. Such events can be rejected by demanding that the missing energy vector **not** point down the beampipe and that the photons are not back-to-back in the azimuthal plane.

4 Conclusions

We have calculated event rates and kinematic distributions for the Standard Model production of two photons plus missing mass through the process $e^+e^- \rightarrow \gamma\gamma\nu\bar{\nu}$ at LEP with beam energies $\sqrt{s}=161, 172, 184,$ and 194 GeV.

In particular, the calculation includes important contributions from W boson exchange when $\nu = \nu_e$. After applying a missing mass M cut of 100 GeV and an angular acceptance cut $|\cos\theta| < .7$, the integrated cross section is fairly independent of the beam energy. For a minimum photon energy of 1.75, 5, and 10 GeV, the expected rate is .016, .007, and .003 pb, respectively. These rates are approximately doubled after including the effect of undetected initial state photon radiation. The photon energies are highly correlated when one or both are soft, but uncorrelated when both are hard. The kinematic region with a large M and two hard photons appears ideal to search for non-Standard Model physics, such as supersymmetry with a higgsino-like or gravitino LSP.

Acknowledgements

We thank G.L. Kane for encouragement in presenting these results, and G.L.K. and G. Mahnon for comments. This work was supported by DOE grant W-31-109-ENG-38.

References

- [*] Electronic mail: mrenna@hep.anl.gov
- [1] J. Amundson, *et al.*, (The Snowmass Supersymmetry Theory Working Group), preprint hep-ph/9609374 (1996).
- [2] S. Ambrosanio, *et al.*, Phys. Rev. Lett. **76**, 3498 (1996).
- [3] S. Dimopoulos, *et al.*, Phys. Rev. Lett. **76**, 3494 (1996); D.R. Stump, *et al.*, Phys. Rev. **D54**, 1936 (1996).
- [4] J.L. Lopez, *et al.*, Phys. Rev. Lett. **77**, 5168 (1996); S. Ambrosanio, *et al.*, preprint hep-ph/9703211 (1997); G.L. Kane and G. Mahlon, preprint hep-ph/9704450 (1997).
- [5] H. Murayama, *et al.*, preprint KEK-91-11 (1992).
- [6] T. Stelzer and W.F. Long, Comput. Phys. Commun. 81, 357 (1994).
- [7] G. Alexander, *et al.*, (The OPAL collaboration), Phys. Lett. **B377**, 222 (1996); K. Ackerstaff, *et al.* (The OPAL collaboration), Phys. Lett. **B391**, 210 (1997).
- [8] S. Ambrosanio, webpage <http://feynman.physics.lsa.umich.edu/~ambros/Phys/2Photon+Emiss/>; see also S. Ambrosanio, *et al.*, Phys. Rev. **D54**, 5395 (1996), and S. Ambrosanio, *et al.*, preprint hep-ph/9703211.

- [9] R. Kleiss, *et al.*, publication CERN 89-08, Vol. 3, p. 143.
- [10] T. Sjöstrand, *Comp. Phys. Commun.* **82**, 74 (1994).

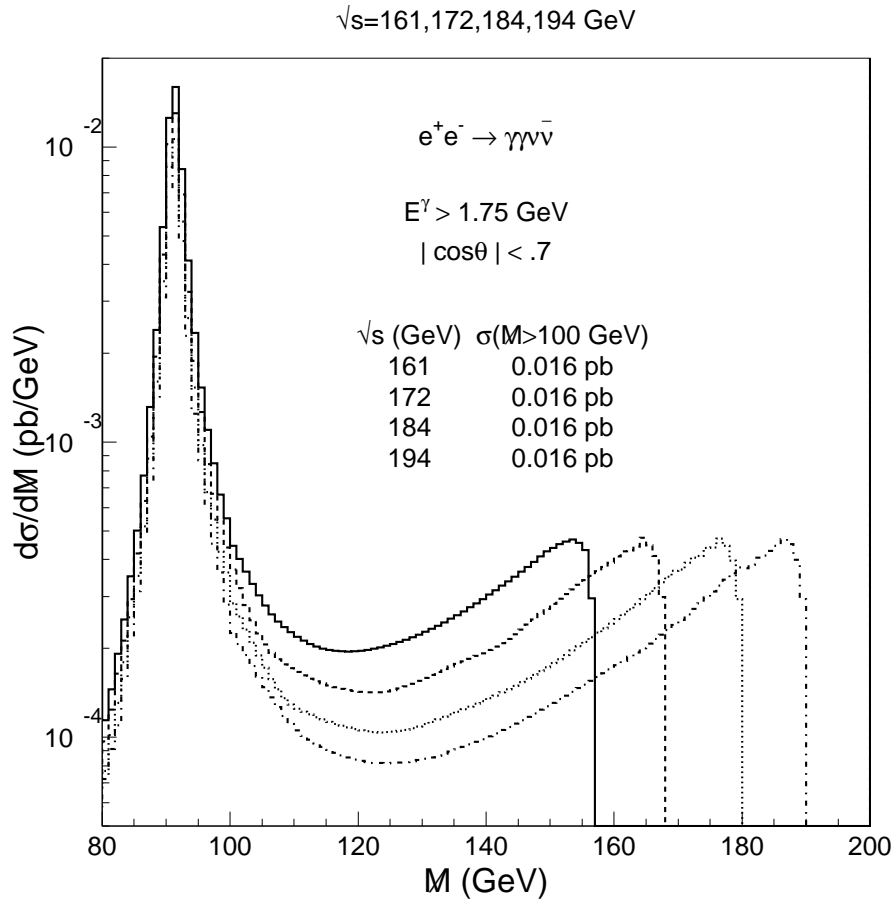


Figure 1: The Missing Mass distribution in pb per GeV bin for a minimum photon energy of 1.75 GeV and $|\cos\theta| < .7$ at $\sqrt{s}=161, 172, 184,$ and 194 GeV. The integrated cross section above 100 GeV is also shown.

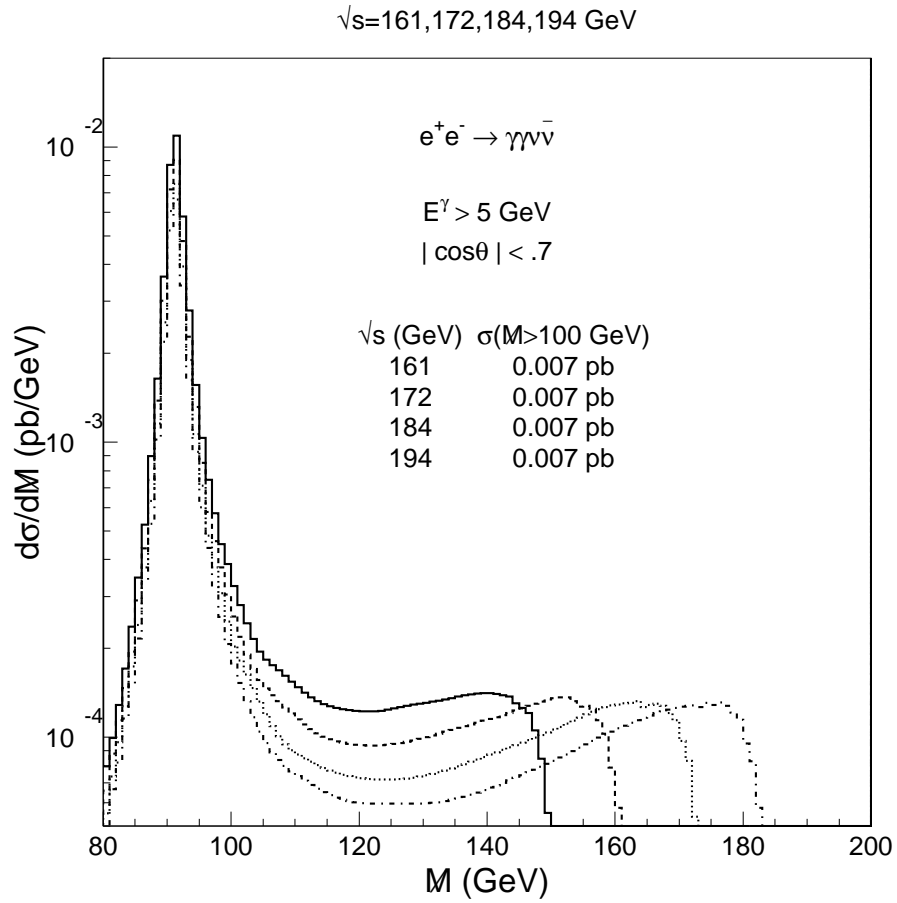


Figure 2: The Missing Mass distribution in pb per GeV bin for a minimum photon energy of 5 GeV and $|\cos\theta| < .7$ at $\sqrt{s}=161, 172, 184,$ and 194 GeV. The integrated cross section above 100 GeV is also shown.

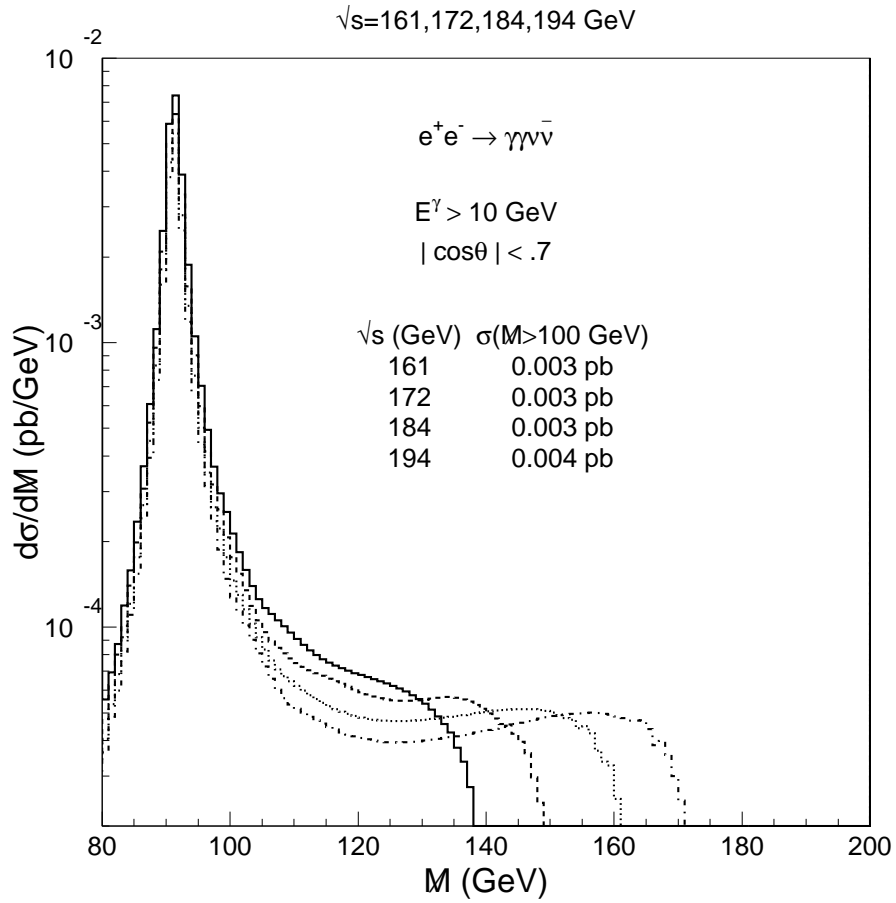


Figure 3: The Missing Mass distribution in pb per GeV bin for a minimum photon energy of 10 GeV and $|\cos\theta| < .7$ at $\sqrt{s}=161, 172, 184,$ and 194 GeV. The integrated cross section above 100 GeV is also shown.

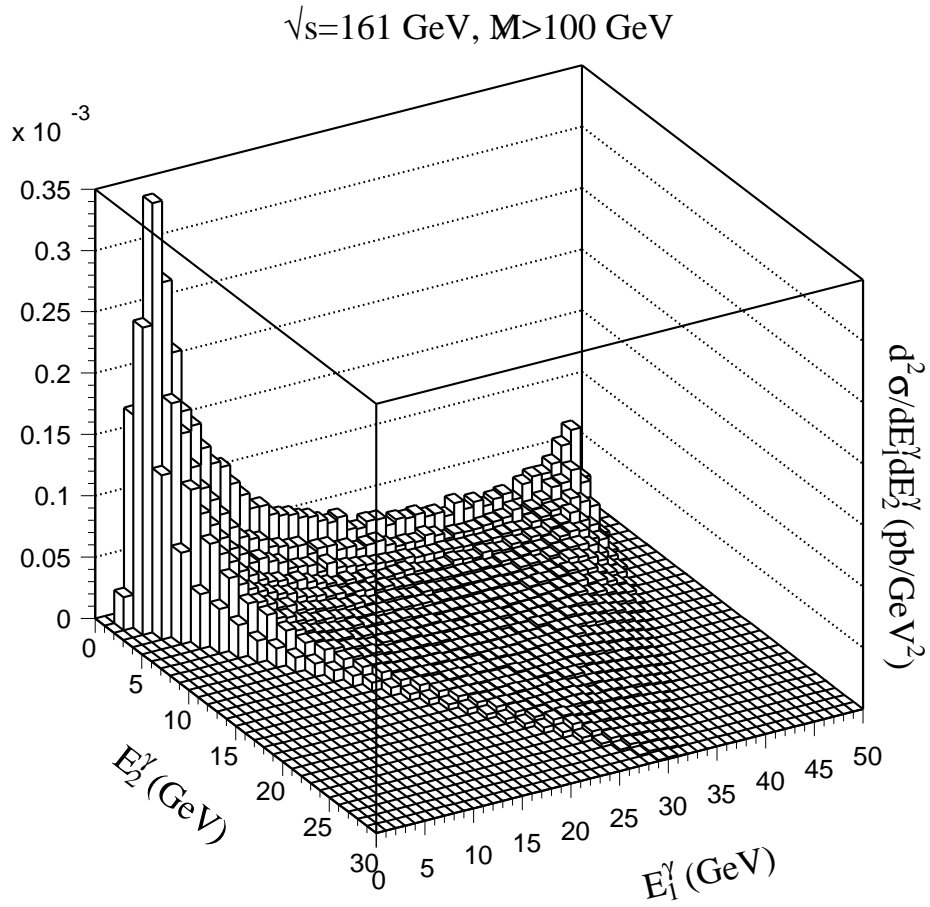


Figure 4: The correlation between the two photon energies in pb per GeV^2 bin at $\sqrt{s}=161 \text{ GeV}$ when $M > 100 \text{ GeV}$. Both photons must satisfy $|\cos \theta| < .7$.

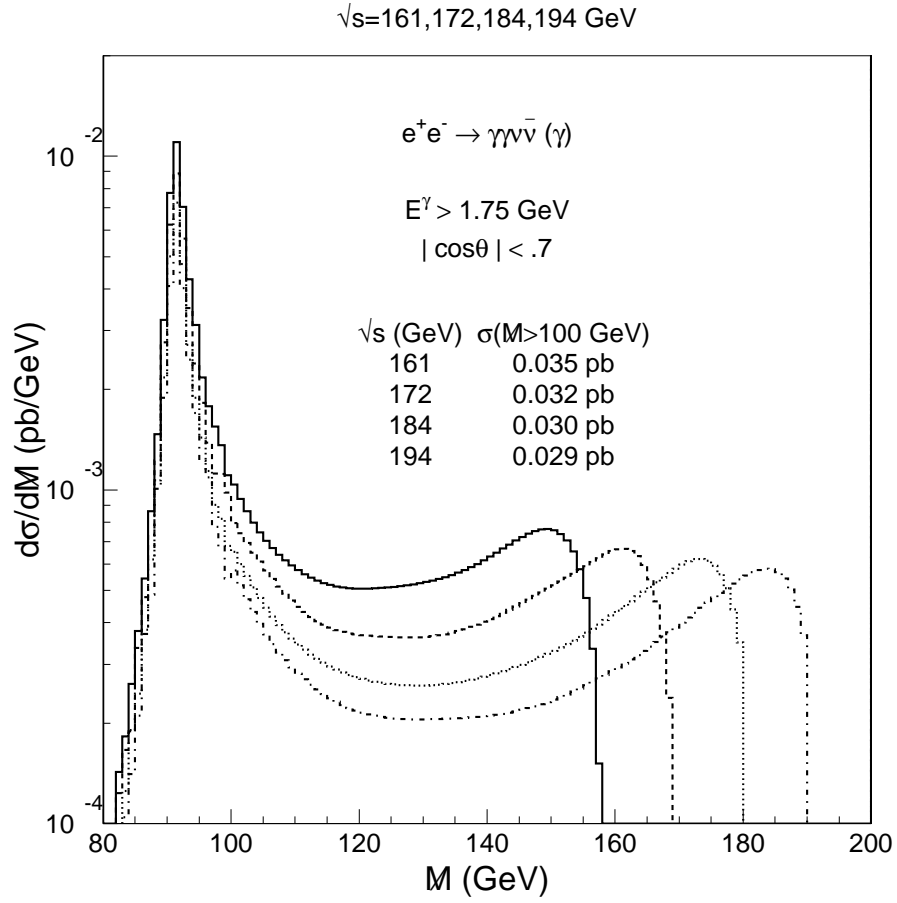


Figure 5: The Missing Mass distribution in pb per GeV bin for a minimum photon energy of 1.75 GeV and $|\cos\theta| < .7$ at $\sqrt{s}=161, 172, 184,$ and 194 GeV. The integrated cross section above 100 GeV is also shown. The effect of undetected initial state radiation has been included.

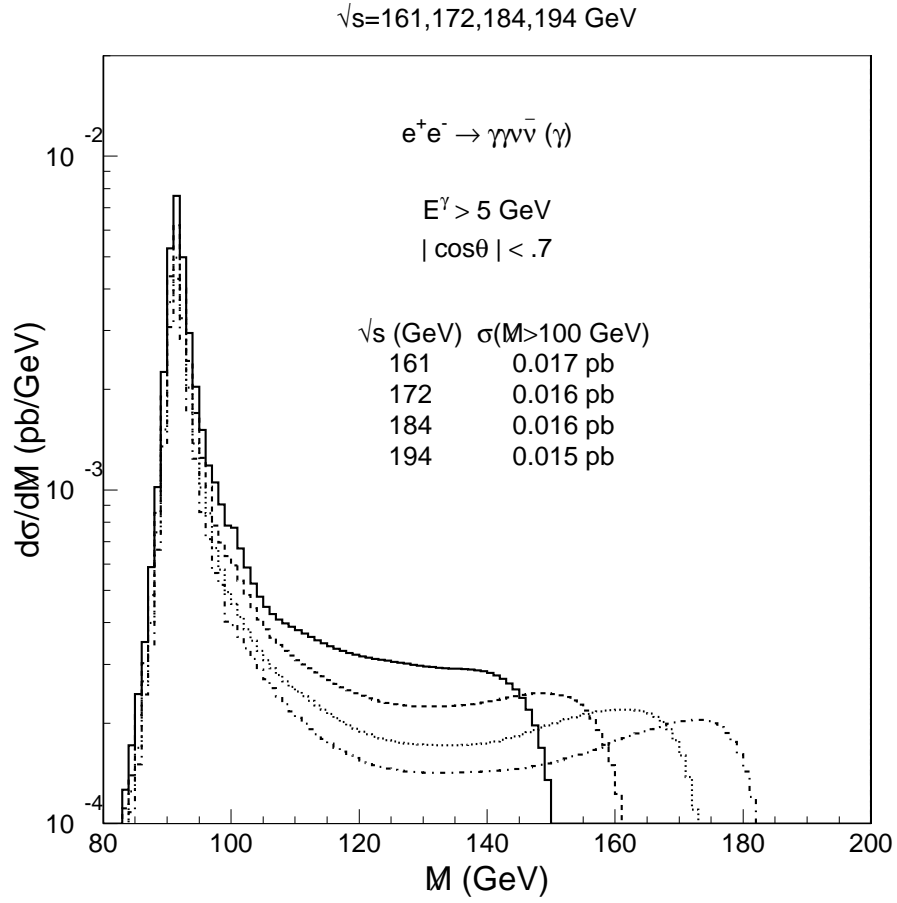


Figure 6: The Missing Mass distribution in pb per GeV bin for a minimum photon energy of 5 GeV and $|\cos\theta| < .7$ at $\sqrt{s}=161, 172, 184,$ and 194 GeV. The integrated cross section above 100 GeV is also shown. The effect of undetected initial state radiation has been included.

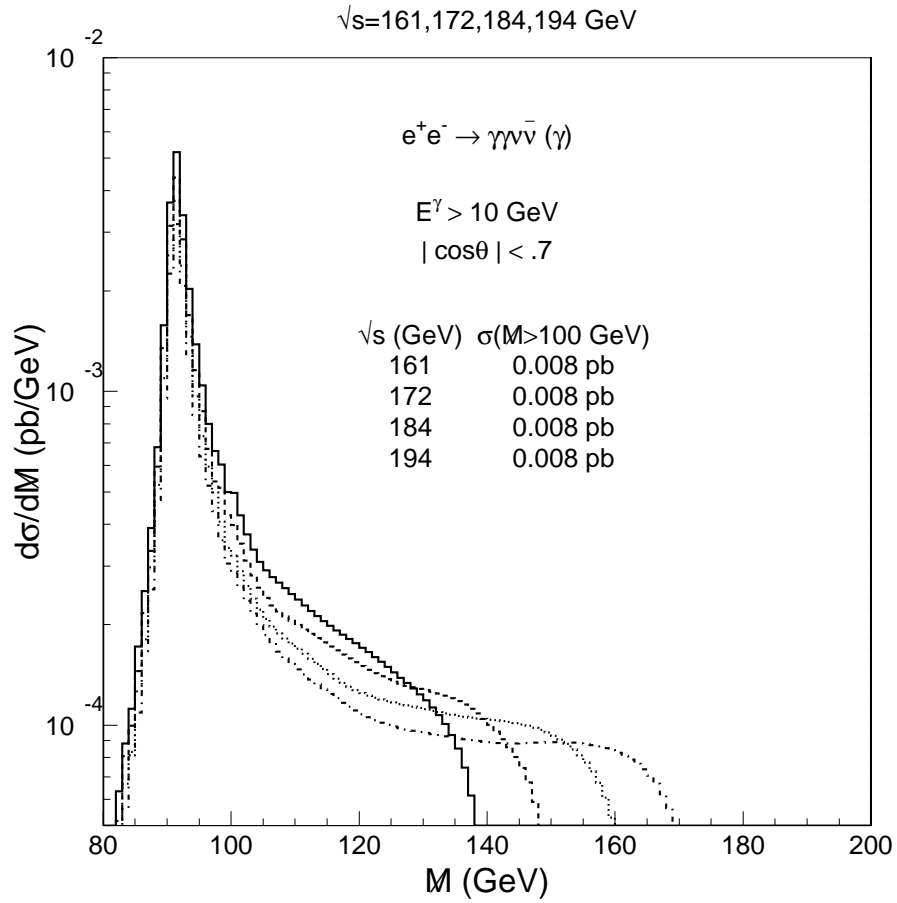


Figure 7: The Missing Mass distribution in pb per GeV bin for a minimum photon energy of 10 GeV and $|\cos\theta| < .7$ at $\sqrt{s}=161, 172, 184,$ and 194 GeV. The integrated cross section above 100 GeV is also shown. The effect of undetected initial state radiation has been included.

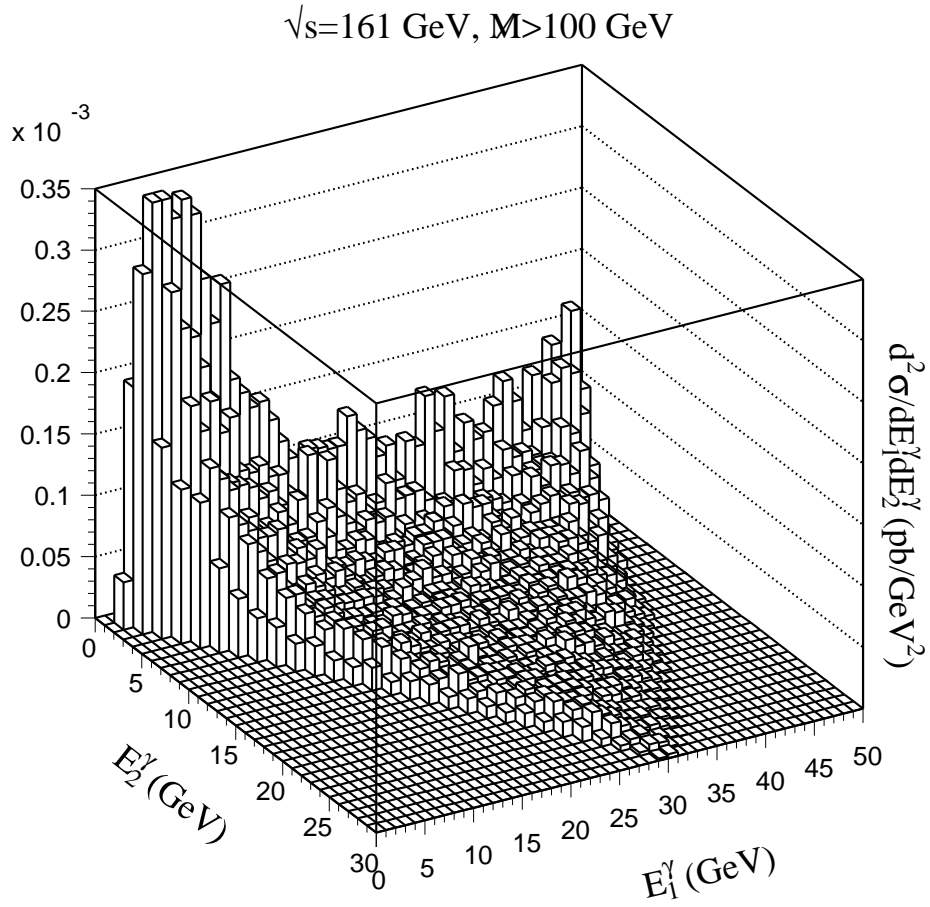


Figure 8: The correlation between the two photon energies in pb per GeV^2 bin at $\sqrt{s}=161 \text{ GeV}$ when $M > 100 \text{ GeV}$. Both photons must satisfy $|\cos\theta| < .7$. The effect of undetected initial state radiation has been included.